Calcium-Induced Refolding of the Calmodulin V136G Mutant Studied by NMR Spectroscopy: Evidence for Interaction between the Two Globular Domains†

Sandrine Fefeu,‡ Rodolfo R. Biekofsky,‡ John E. McCormick,‡ Stephen R. Martin,§ Peter M. Bayley,§ and James Feeney*,‡

Molecular Structure Division and Physical Biochemistry Division, National Institute for Medical Research, Mill Hill, London NW7 1AA, U.K.

Received July 28, 2000; Revised Manuscript Received October 17, 2000

ABSTRACT: The Ca^{2+} titration of the ^{15}N-labeled mutant V136G calmodulin has been monitored using $^{1}H-^{15}N$ HSQC NMR spectra. Up to a $[Ca^{2+}]/[CaM]$ ratio of 2, the Ca^{2+} ions bind predominantly to sites I and II on the N-domain in contrast with the behavior of the wild-type calmodulin where the C-terminal domain has the higher affinity for Ca^{2+}. Surprisingly, the Ca^{2+}-binding affinity for the N-domain in the mutant calmodulin is greater than that for the N-domain in the wild-type protein. The mutated C-domain is observed as a mixture of unfolded, partially folded (site III occupied), and native-like folded (sites III and IV occupied) conformations, with relative populations dependent on the $[Ca^{2+}]/[CaM]$ ratio. The occupancy of site III independently of site IV in this mutant shows that the cooperativity of Ca^{2+} binding in the C-domain is mediated by the integrity of the domain structure. Several NH signals from residues in the Ca^{2+}-bound N-domain appear as two signals during the Ca^{2+} titration indicating separate species in slow exchange, and it can be deduced that these result from the presence and absence of interdomain interactions in the mutant. It is proposed that an unfolded part of the mutated C-domain interacts with sites on the N-domain that normally bind to target proteins. This would also account for the increase in the Ca^{2+} affinity for the N-domain in the mutant compared with the wild-type calmodulin. The results therefore show the wide-ranging effects of a point mutation in a single Ca^{2+}-binding site, providing details of the involvement of individual residues in the calcium-induced folding reactions.

Calmodulin (CaM)[1] is a calcium-binding protein that mediates many calcium-induced intracellular regulatory events (*1*, *2*). Extensive structural information has been obtained for calmodulin in its Ca^{2+}-free (apo) and Ca^{2+}-bound (holo) forms and for its complexes with target peptides (*3*, *4*). The X-ray diffraction structure of Ca_4-CaM revealed a dumbell-shaped molecule, with its N- and C-terminal domains (containing residues 1−75 and 76−148, respectively) separated by a long interconnecting helix (*5*). Subsequent solution NMR studies showed that the interconnecting sequence had considerable flexibility, and hence the domains can adopt different positions with respect to each other (*6*). Each globular domain contains two high-affinity Ca^{2+}-binding sites of the EF-hand (helix−loop−helix) type (*7*). The first two Ca^{2+} ions bind to the C-domain (sites III and IV), and the second two Ca^{2+} ions bind to the N-domain (sites I and II) (*8*). The Ca^{2+}-saturated form of CaM (holo) is conformationally distinct from the Ca^{2+}-free form (apo) (*9*−*11*). Activation of the majority of CaM-dependent proteins requires Ca^{2+} ions. Saturation of the calcium-binding sites induces conformational changes in both domains that enable CaM to recognize and bind a multiplicity of target peptides and proteins with high affinity (*4*, *12*, *13*). Interaction of CaM with target sequences exploits the intrinsic flexibility of the interdomain sequence to give complexes with relatively compact structures, as reviewed by Crivici and Ikura (*4*). Enzyme activation by CaM generally appears to involve Ca^{2+} binding by both of its domains, although a sequential domain-specific binding is seen in target interactions (*13*) and in the interaction with skeletal muscle myosin light chain kinase (*14*).

Previous studies on calmodulin and related proteins have demonstrated the importance of hydrophobic interactions in calmodulin folding and calmodulin−peptide complex formation. The mutation of certain key residues can reveal important structure−function−evolution features of a protein and also provides an indirect way of probing interactions of conserved residues and their effects on protein folding. The availability of engineered calmodulins (*15*, *16*) has allowed elucidation of different aspects of the dynamics and energetics of Ca^{2+} binding (*17*−*23*) as well as the different modes of recognition and complex formation found in different types of mutants and target peptides (*24*−*28*). Recently, the

† This work was supported by funds from the Medical Research Council. S.F. acknowledges the award of a European Marie Curie Fellowship.

* To whom correspondence should be addressed: fax +44 208 906 4477; phone +44 208 959 3666; e-mail jfeeney@nimr.mrc.ac.uk.

‡ Molecular Structure Division.

§ Physical Biochemistry Division.

[1] Abbreviations: CaM, calmodulin; CaM(V136G), calmodulin mutant replacing Val136 with Gly; CD, circular dichroism; HSQC, heteronuclear single-quantum coherence spectroscopy; NMR, nuclear magnetic resonance; NOE, nuclear Overhauser effect; NOESY, nuclear Overhauser effect spectroscopy; ROESY, rotating frame nuclear Overhauser effect spectroscopy; sk-MLCK, skeletal muscle myosin light chain kinase; sm-MLCK, smooth muscle myosin light chain kinase; TOCSY, total correlation spectroscopy; 2D, two dimensional; 3D, three dimensional.

10.1021/bi001772a CCC: $19.00
Published on Web 12/02/2000

stabilities of CaMs with single point mutations at position 8 of each of the four calcium-binding loop sequences (sites I, II, III, and IV) have been studied by fluorescence and circular dichroism (*29*). Position 8 of each 12-residue calcium-binding loop is a well-conserved isoleucine or valine residue. These highly conserved residues are part of the hydrophobic core of either calmodulin domain and are involved in a structural link between the pair of calcium-binding sites in each domain formed via a short antiparallel β-sheet. Hydrogen bonds between position 8 residues on the Ca^{2+}-binding loops in sites I and II on one hand, and between corresponding residues in sites III and IV on the other, contribute to the stability of the structure of each pair of Ca^{2+}-binding loops. For the position 8 mutants where the isoleucine or valine is replaced by glycine, the mutation in site IV (residue 136) has a much larger effect on the thermal stability of the protein than does the corresponding mutation in site I, II, or III (residues 27, 63, and 100, respectively). CD measurements showed that the loss of secondary structure of the apo proteins could be completely restored by Ca^{2+} binding for the calmodulins with single-point mutations in site I, II, or III, but this was not the case for the site IV mutation. The addition of Ca^{2+} does not cause full recovery of the secondary structure of CaM(V136G) even though the stoichiometric association constants for Ca^{2+} binding to this mutant are similar to those of the wild-type CaM (*29*, *30*).

The present work describes NMR studies of the Ca^{2+}-induced conformational changes for calmodulin with a V136G mutation in position 8 of the site IV calcium-binding loop with the aim of elucidating the effect of this mutation on the conformation of the C-domain and the origins of the Ca^{2+}-induced refolding behavior for this site IV mutant. As part of this study, a Ca^{2+} titration of the ^{15}N-labeled apo mutant V136G CaM was carried out. Previous work had shown that site-specific binding of Ca^{2+} to each of the four Ca^{2+}-binding sites of CaM can be monitored using $^1H-^{15}N$ HSQC NMR measurements (*30*). The results reported here show key features of the effects of the V136G mutation on the structure, stability, and function of calmodulin as well as revealing interesting insights into the folding−unfolding process, the intradomain cooperativity for the calcium binding, and interactions between the domains. Several recent publications have drawn attention to interdomain interactions in various CaMs (*31*−*38*). In particular, in the case of yeast CaM, where there is a defective fourth Ca^{2+}-binding site, an interdomain interaction modulating the overall conformation and its function has been recently postulated (*37*, *38*). This gives particular relevance to the present results for the V136G CaM mutant, which also has a defective fourth Ca^{2+}-binding site.

MATERIALS AND METHODS

Protein Expression and Purification. Drosophila melanogaster wild-type CaM and the CaM(V136G) mutant were expressed in *Escherichia coli* and purified as described previously (*26*, *29*, *30*). The uniformly ^{15}N-labeled proteins were made by incorporating 99% ^{15}N-labeled $(NH_4)_2SO_4$ as the sole nitrogen source into the growth media. A sample of selectively ^{15}N-Ile-labeled CaM(V136G) was prepared by incorporating 97% ^{15}N-Ile into a growth media containing a defined mixture of all of the other unlabeled amino acids. The purities of the CaM samples were monitored by NMR, mass spectroscopy, and UV measurements. The ^{15}N-labeled protein samples used for the NMR studies were 0.77−1.20 mM solutions of protein in 90% H_2O/10% D_2O and 0.1 M KCl. The pH of the sample was adjusted to 6.8 (uncorrected for deuterium isotope effects).

Peptide. A 26-residue peptide encompassing the calmodulin-binding region of the skeletal myosin light chain kinase (sk-MLCK) (NH_2-KRRWKKNFIAVSAANRFK-KISSSGAL-CO_2H) was purchased from the Department of Biochemistry, Bristol University. The purity of the sample was checked with mass spectroscopy.

NMR Spectroscopy. The nuclear magnetic resonance experiments were performed on a Varian Inova 600 spectrometer over a temperature range of 1−45 °C. Water suppression was achieved using the WaterGate sequence (*39*) in all of the NMR experiments. 2D $^1H-^{15}N$ HSQC spectra were recorded at 25 °C typically using 2048 × 64 data points. 2D $^1H-^{15}N$ HSQC−ROESY and 3D ROESY−HSQC (*39*) spectra were recorded at 25 °C in the phase-sensitive mode with a spin-lock time of 45ms and using 1024 × 128 × 64 complex data points. 3D NOESY−HSQC and TOCSY−HSQC spectra (*39*) were acquired at 25 °C for the holo and apo CaM(V136G) samples. The heteronuclear NOE spectra were acquired using the method described by Kay et al. (*40*). Spectra were processed using NMRPipe (*41*) and analyzed using NMRDraw (sofware written by F. Delaglio) and Felix98.0 sofware (MSI Inc.). The NMR signal assignments for the mutant CaM(V136G) were made by analyzing 3D NOESY−HSQC and 3D TOCSY−HSQC spectra and by comparison with the known assignments for the wild-type apo-CaM (M. Ikura, personal communication) and holo-CaM (*42*, *43*).

Ca^{2+} Titrations. A stock solution of 45 mM $CaCl_2$ in 90% H_2O/10% D_2O was prepared by dilution from a standard volumetric solution (Merck). The Ca^{2+} titrations were carried out by monitoring amide NH signals in $^1H-^{15}N$ HSQC NMR spectra recorded at 25 °C. For each titration point the required aliquot of this stock $CaCl_2$ solution was added to the NMR tube containing the calmodulin solution and mixed thoroughly. Allowance was made for dilution effects on adding the Ca^{2+} solution. The initial concentrations of mutant CaM were 1.20 and 0.77 mM for the uniformly and selectively ^{15}N-labeled samples, respectively [the protein concentration was calculated using $\epsilon_{259} = 2203\ M^{-1}\ cm^{-1}$ (*29*)]. A good estimate of the $[Ca^{2+}]/[CaM] = 2$ ratio could also be made from the NMR spectra monitoring the stoichiometric titration of Ca^{2+} into the N-domain binding sites of the mutant CaM. The addition of Ca^{2+} to the NMR sample did not cause significant changes in the pH of the sample. The Ca^{2+} titrations were repeated twice. The signal volumes were calculated by using the optimization procedure for measuring volumes in Felix98.0 sofware (MSI Inc.).

RESULTS

Mutant CaM(V136G) in the Absence of Ca^{2+}. The $^1H-^{15}N$ HSQC NMR spectrum for the ^{15}N-labeled CaM(V136G) mutant in the absence of Ca^{2+} (apo) was acquired at 25 °C and compared with the corresponding spectrum of apo wild-type calmodulin. This comparison reveals that many of the signals from C-domain residues in the two proteins have very different chemical shifts while those from the N-domain

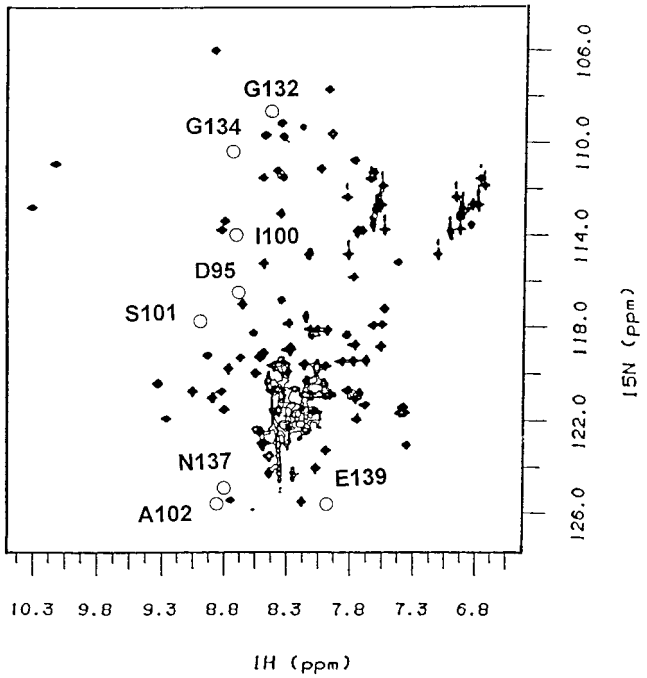

FIGURE 1: 2D $^1H-^{15}N$ HSQC spectra at 25 °C in the absence of calcium for the uniformly ^{15}N-labeled mutant CaM(V136G). The positions of some of the apo wild-type CaM displaced signals are indicated on the spectrum.

residues are relatively unperturbed. Figure 1 shows the spectrum for the apo-CaM(V136G) mutant with the positions of some of the displaced C-domain signals from apo wild-type CaM indicated on the spectrum. The affected signals include those from residues D95, I100, S101, and A102 from the site III binding loop and residues G132, G134, N137, Y138, and E139 from the site IV binding loop. The $^1H-^{15}N$ HSQC spectrum of the CaM mutant also shows several narrow resonances at positions characteristic of unfolded residues. Measurements of heteronuclear Overhauser effects showed that these signals arise from nuclei having the greatest mobility and are typical of residues in unstructured mobile regions of the protein. The $^1H-^{15}N$ HSQC spectrum of the apo mutant CaM prepared with selective ^{15}N-Ile labeling indicated that while the four Ile residues in the N-domain have chemical shifts expected for wild-type CaM, the four Ile residues in the C-domain have very different chemical shifts from those of the wild type with values typical of unfolded residues. Two of the latter residues are in the Ca^{2+}-binding sites III and IV (Ile100 and Ile130) and two are in helices (Ile85 and Ile125).

From this analysis, it can be concluded that the N-domain of the mutant CaM retains the fold found in wild-type apo-CaM, while the C-domain does not [its Ca^{2+}-binding sites III and IV being unfolded as well as some of its helical structure (species A in Scheme 1)]. Upon addition of Ca^{2+}, part of the C-domain becomes refolded, and 2D exchange experiments have been used to assign the narrow signals to specific unfolded residues by connecting them with assigned signals in the folded C-domain by magnetization transfer (see later).

Occupancy of EF-Hand Calcium-Binding Sites in Mutant CaM(V136G). The sensitivity of ^{15}N chemical shifts of specific residues to the binding of calcium to EF-hand loops allows a Ca^{2+} titration using 2D $^1H-^{15}N$ HSQC NMR spectra

Scheme 1: Schematic Representation of Species A−D Detected by $^1H-^{15}N$ HSQC Experiments in the Calcium-Induced Refolding of the CaM(V136G) Mutant[a]

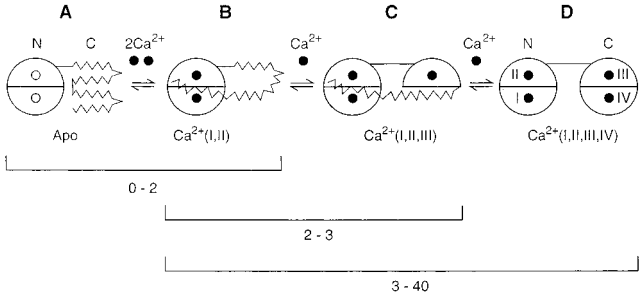

[a] The hemispherically shaped segments indicate intact Ca^{2+}-binding sites, and the zigzag segments indicate unfolded Ca^{2+}-binding sites. An interdomain interaction is indicated by a zigzag segment overlapping the hemispherically shaped segments. Species A corresponds to the apo form, B and C represent species with partial Ca^{2+} occupation, and D is a species with full Ca^{2+} occupation. The numbers under the bars refer to the ranges of $[Ca^{2+}]/[CaM]$ ratios for which these species were detected.

of the ^{15}N-labeled CaM(V136G) mutant to be used to monitor the Ca^{2+} occupancy of the different sites (*30*). Particular attention has been focused on the residues in position 8 of the EF-hand loops of calmodulin. The amide NH group of residue 8 is part of the peptide bond formed with the carbonyl group of the position 7 residue, and this is the only backbone carbonyl directly involved in binding to a Ca^{2+} ion. The coordination of the calcium ion to this carbonyl group results in large deshielding effects of the position 8 backbone amide ^{15}N nucleus, thus allowing its ^{15}N shift to be used as a sensitive probe of site-specific Ca^{2+} binding (*30*). In CaM(V136G), the position 8 residues are Ile27 and Ile63 for sites I and II in the N-domain and Ile100 and Gly136 for sites III and IV in the C-domain, respectively. Using the fact that three of these four residues are isoleucines, a Ca^{2+} titration using 2D $^1H-^{15}N$ HSQC NMR spectra on a sample of CaM(V136G) mutant containing selectively ^{15}N-labeled isoleucine residues has also been carried out. This sample was particularly useful for monitoring the Ile27, Ile63, and Ile100 residues because in some cases their NH signals overlap other signals in spectra obtained with uniformly ^{15}N-labeled samples.

The NMR spectral changes for Ile27 and Ile63 (sites I and II) occur in moderately slow exchange on the NMR chemical shift time scale leading to separate signals corresponding to Ca^{2+}-bound and Ca^{2+}-free species (^{15}N shift differences of 16.55 and 4.73 ppm for Ile27 and Ile63, respectively). This behavior contrasts with that of wild-type calmodulin, for which the NMR spectral changes for Ile27 and Ile63 occur in moderately fast exchange on the NMR chemical shift time scale leading to signals with averaged chemical shifts for the nuclei exchanging between Ca^{2+}-bound and Ca^{2+}-free species but with contributions to their line widths from the exchange process (*44*). The difference in exchange behavior for the N-domain sites between wild-type and mutant calmodulins is surprising since their N-domains are identical (as are the Ca^{2+}-induced shifts). The different behavior can be seen in Figure 2, which shows the NH signals for Ile63 in the $^1H-^{15}N$ HSQC spectra recorded at different $[Ca^{2+}]/[CaM]$ ratios for apo wild-type CaM (Figure 2A) and for the apo-CaM(V136G) mutant (Figure 2B).

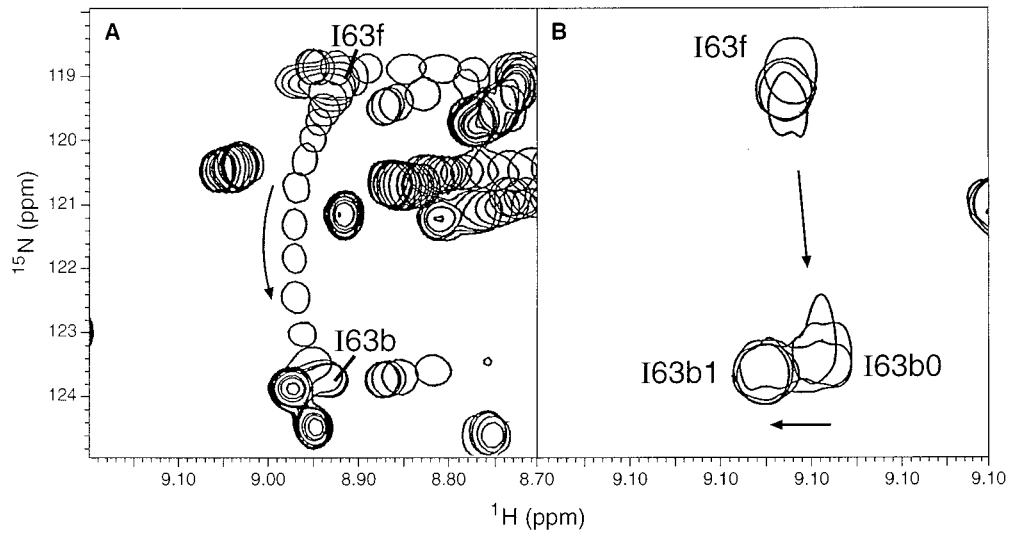

FIGURE 2: Contour plots of the Ile63 signals in the 2D $^{1}H-^{15}N$ HSQC NMR spectrum recorded at $[Ca^{2+}]/[CaM]$ ratios between 0 and 5 for (A) ^{15}N-labeled wild-type CaM showing fast exchange and (B) [^{15}N-Ile]-CaM(V136G) showing moderately slow exchange. Two forms (I63b0 and I63b1) were observed for the Ca^{2+}-bound form of the mutant CaM(V136G) at a $[Ca^{2+}]/[CaM]$ ratio of 2. The data for (A) was taken from ref *30*.

The NMR spectral changes for Ile100 and Gly136 (sites III and IV, respectively) for the mutant CaM also occur in slow exchange on the NMR chemical shift time scale leading to separate signals corresponding to two C-domain Ca^{2+}-bound species [Ca^{2+}(I, II, III) and Ca^{2+}(I, II, III, IV)] and a C-domain Ca^{2+}-free species [Ca^{2+}(I, II)]. The mutant C-domain Ca^{2+}-free species appear to be mostly unfolded (as discussed above), whereas the C-domain Ca^{2+}-bound species with both sites occupied appears to be folded since the signals for certain residues in calcium-binding sites III and IV are found at spectral positions similar to those in the spectrum of Ca^{2+}-bound wild-type CaM. As with the behavior observed for Ile100 and Val136 in the wild-type CaM, the ^{15}N nuclei for Ile100 and Gly136 are greatly deshielded upon Ca^{2+} binding to sites III and IV of the mutant calmodulin. The C-domain of the Ca^{2+}-bound species with only site III occupied is partially unfolded. The Ile100 signal monitoring the Ca^{2+} binding at site III for this latter species has been assigned by magnetization transfer experiments with the previously assigned Ile100 signal in the Ca_4-CaM species (see later).

The data analysis involved measuring the volume of each peak of interest at each point in the titration. The volumes of the signals from residues in position 8 of EF-hand loops in sites I, II, III, and IV of Ca^{2+}-bound calmodulin were measured, and the changes in volume were normalized and plotted as a function of the $[Ca^{2+}]/[CaM]$ ratio (see Figure 3). An outstanding feature observed in the $^{1}H-^{15}N$ HSQC NMR Ca^{2+} titration spectra of the CaM(V136G) mutant is the appearance of signals for different Ca^{2+}-bound species in slow exchange (see below). In particular, at $[Ca^{2+}]/[CaM]$ ratios between 3 and 18, Ile27 and Ile100 each show two Ca^{2+}-bound signals (namely, Ile27b1 and Ile27b2, Ile100b1 and Ile100b2) (see Figures 4 and 5). The Ile100b1 signals correspond to the Ca_3-CaM species C with sites I, II, and III occupied, and the Ile100b2 signal corresponds to the folded Ca_4-CaM species D with its site IV binding loop in the wild-type-like conformation. For Ile27 and Ile63 the b1 signal also includes the Ca_2-CaM species B with only sites I and II occupied. The sums of the volumes of the position 8 Ca^{2+}-bound signals for the different species were used in order to plot occupancy curves for each calcium-binding site at different calcium concentrations.

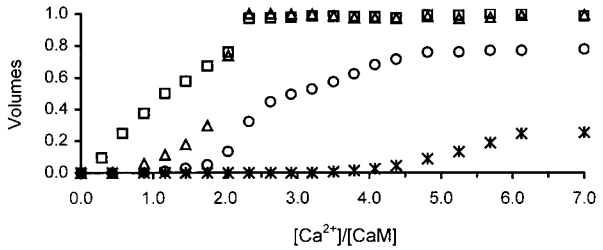

FIGURE 3: Calcium occupancy of EF-hand calcium-binding sites for the mutant CaM(V136G) obtained from the Ca^{2+} titration $^{1}H-^{15}N$ HSQC spectra. Site I is from Ile27 (△), site II from Ile63 (□), site III from Ile100 (○), and site IV from Gly136 (∗). The values are the sums of the normalized volumes of the position 8 signals for the different Ca^{2+}-bound species as reported in Figure 4. For residues Ile27, Ile63, and Ile100, the signal volumes were measured from the spectra of the ^{15}N-Ile-labeled CaM(V136G) and for the residue Gly136 from the spectra of the uniformly ^{15}N-labeled CaM-(V136G). The curves are normalized according to $I_{obs}/(I_{total})_{max}$ for residues Ile27 and Ile63. The normalization of the Ile100 and Gly136 signals is described in the text.

Figure 3 shows the normalized calcium occupancy curves for sites I, II, III, and IV as a function of the $[Ca^{2+}]/[CaM]$ ratios. The curves corresponding to signals from N-domain sites I and II (Ile27 and Ile63, respectively) increase steeply between $[Ca^{2+}]/[CaM]$ ratios of 0 and 2, and at a $[Ca^{2+}]/[CaM]$ ratio of 2 each shows a site occupation approaching 100%. This behavior contrasts strongly with that observed in $^{1}H-^{15}N$ HSQC spectra of wild-type CaM where added Ca^{2+} first perturbs Ile100 and Val136 in the C-domain sites III and IV (*8*, *30*, and references therein). For the mutant CaM, the curves corresponding to signals from the C-domain sites III and IV (Ile100 and Gly136, respectively) increase gradually as the calcium is added and not in a parallel fashion, with site III binding Ca^{2+} ions before site IV. The curve corresponding to site III starts at a $[Ca^{2+}]/[CaM]$ ratio of ∼2 and at a $[Ca^{2+}]/[CaM]$ ratio of 7 reaches 80 ± 10% of full site III occupation. The occupation of site III was estimated by considering the Ile100b1/Ile100b2 and Ile27b1/

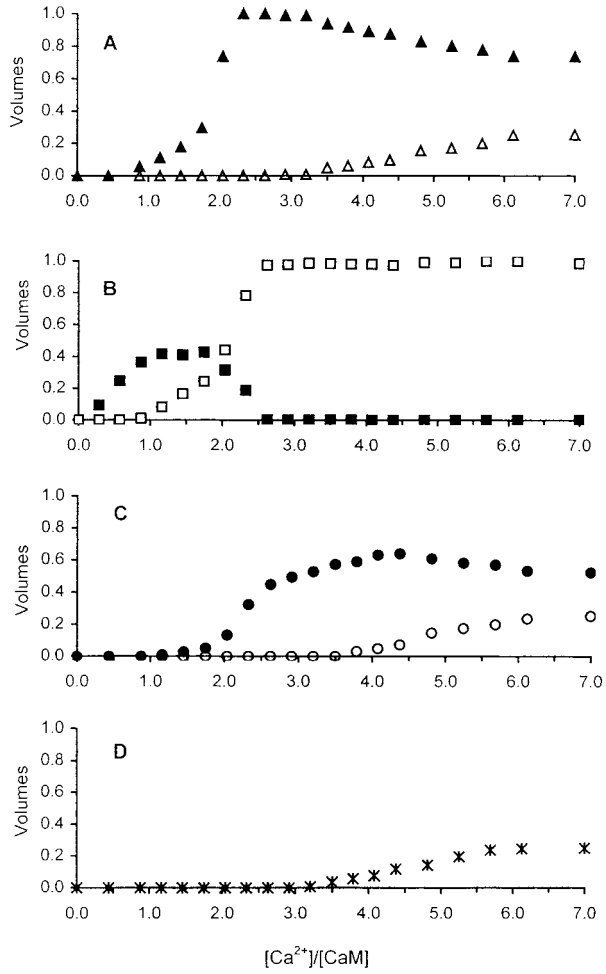

FIGURE 4: Calcium titration plots (25 °C) for Ile27b1 (▲), Ile27b2 (△), Ile63b0 (■), Ile63b1 (□), Ile100b1 (●), Ile100b2, (○), and Gly136b (∗) with the normalized volumes monitoring the relative concentrations of the different Ca^{2+}-bound species. For residues Ile27, Ile63, and Ile100, the signal volumes were measured from the spectra of the ^{15}N-Ile-labeled CaM(V136G) and for the residue Gly136 from the spectra of the uniformly ^{15}N-labeled CaM(V136G). For the N-domain residues Ile27 and Ile63, the curves were normalized according to $I_{obs}/(I_{total})_{max}$. The normalization of curves for the C-domain residues Ile100 and Gly136 is described in the text. The estimated standard deviations on the volume measurements are ±5%.

Ile27b2 signal intensity ratios (which are proportional to $[p_3/p_4]$ and $[(p_2 + p_3)/p_4]$, respectively, where p_2, p_3, and p_4 are the fractional populations of species with sites I and II, sites I, II, and III, and sites I, II, III, and IV occupied). The curve for Gly136 (shown in Figure 3) corresponding to occupation of site IV starts at a $[Ca^{2+}]$/[CaM] ratio of 3 and at a $[Ca^{2+}]$/[CaM] ratio of 7 reaches 20 ± 10% of site IV occupation. At a $[Ca^{2+}]$/[CaM] ratio of 18 the site IV occupation rises to 55 ± 10% and site III occupation is still incomplete.

Mutant CaM(V136G) Species Present in Solution at Different $[Ca^{2+}]$/[CaM] Ratios. As well as providing an overall view of the calcium-binding behavior of the CaM-(V136G) mutant (see above), the Ca^{2+} titration using 2D ^{1}H−^{15}N HSQC NMR spectra of the ^{15}N-labeled CaM-(V136G) mutant provides information about the exchange between the different species present in solution at different $[Ca^{2+}]$/[CaM] ratios. Figure 4 shows the normalized curves for the position 8 residues from their different Ca^{2+}-bound forms present in solution at different $[Ca^{2+}]$/[CaM] ratios. The different species detected between $[Ca^{2+}]$/[CaM] ratios of 0−40 are shown in Scheme 1.

(i) $[Ca^{2+}]$/[CaM] Ratios between 0 and 2. The changes in the NMR spectra observed when Ca^{2+} was added up to a $[Ca^{2+}]$/[CaM] ratio of 2 were limited almost exclusively to N-domain residues of the protein. Initially, there was only one signal for Ca^{2+}-free Ile63 (Ile63f). Upon addition of calcium, a signal for Ca^{2+}-bound Ile63 (Ile63b0) emerged for a Ca^{2+}-bound conformation at a $[Ca^{2+}]$/[CaM] ratio of 0.3. A second signal for Ca^{2+}-bound Ile63 (Ile63b1) in slow exchange with the previous Ca^{2+}-bound Ile63 (Ile63b0) appeared at a $[Ca^{2+}]$/[CaM] ratio of 1. This signal, at the known position for Ca^{2+}-bound Ile63, continued to increase up to a $[Ca^{2+}]$/[CaM] ratio of 2.2 and then remained constant until the end of the titration. The intensity of the Ile63b0 signal decreased after the Ile63b1 signal emerged and disappeared at a $[Ca^{2+}]$/[CaM] ratio of 2.2. Multiple signals were also observed for other residues of the N-domain. A good example is provided by Gly33 where the NH signal from Gly33 is observed in an isolated region of the spectrum and also showed multiple signals between $[Ca^{2+}]$/[CaM] ratios of 0−2. The fact that N-domain residues present two signals in slow exchange strongly suggests that there is an interaction between the Ca^{2+}-bound N-domain and the extended unfolded conformation of the C-domain (this is also fully consistent with the observed affinity of Ca^{2+} for the N-domain being greater for the mutant protein than for the wild type). By analogy with the wild-type calmodulin behavior, binding calcium to sites I and II of the N-domain in the mutant protein would be expected to change the N-domain conformation from a closed to an open conformation, exposing its hydrophobic core (*4*, *11*). The multiple signals observed for the Ca^{2+}-bound Ile63 could correspond to two conformations of the Ca^{2+}-bound N-domain binding to residues of the unfolded chain of the C-domain (i.e., signals b0 and b1 correspond to two different conformations of species B in Scheme 1). A comparison of the titration curves for Ile27 and Ile63 (see Figure 4A,B) strongly suggests that for Ile27 only one of these species (the b1 signal) has been detected (the Ile27 signals at these $[Ca^{2+}]$/[CaM] ratios are much broader than those for Ile63). Further evidence for this suggestion is that two signals are seen for Gly33 in this part of the titration. It should be noted that the signals for Ile27 above a $[Ca^{2+}]$/[CaM] ratio of ∼2 indicate full occupancy of site I.

(ii) $[Ca^{2+}]$/[CaM] Ratios between 2 and 3. At a $[Ca^{2+}]$/[CaM] ratio of 2, the N-domain sites I and II approached saturation with calcium. At a ratio of 2 a signal had started to emerge for the site III Ca^{2+}-bound Ile100 (Ile100b1) in slow exchange with the apo signal for Ile100 (Ile100f), the signals being connected to each other by observing exchange cross-peaks in the NOESY and ROESY spectra (not shown). This behavior is consistent with the exchange between Ca_2-CaM and Ca_3-CaM species in which the N-domain sites are Ca^{2+} saturated and site III is Ca^{2+} free or Ca^{2+} bound, respectively (species B and C in Scheme 1). The Ile100b1 signal has also been assigned by magnetization transfer experiments with the Ile100b2 signal in the mutant Ca_4-CaM species that has the same chemical shifts as in the wild-type CaM (see Figure 6).

(iii) $[Ca^{2+}]$/[CaM] Ratios between 3 and 40. At a $[Ca^{2+}]$/[CaM] ratio of 3.3 the second signal for calcium-bound

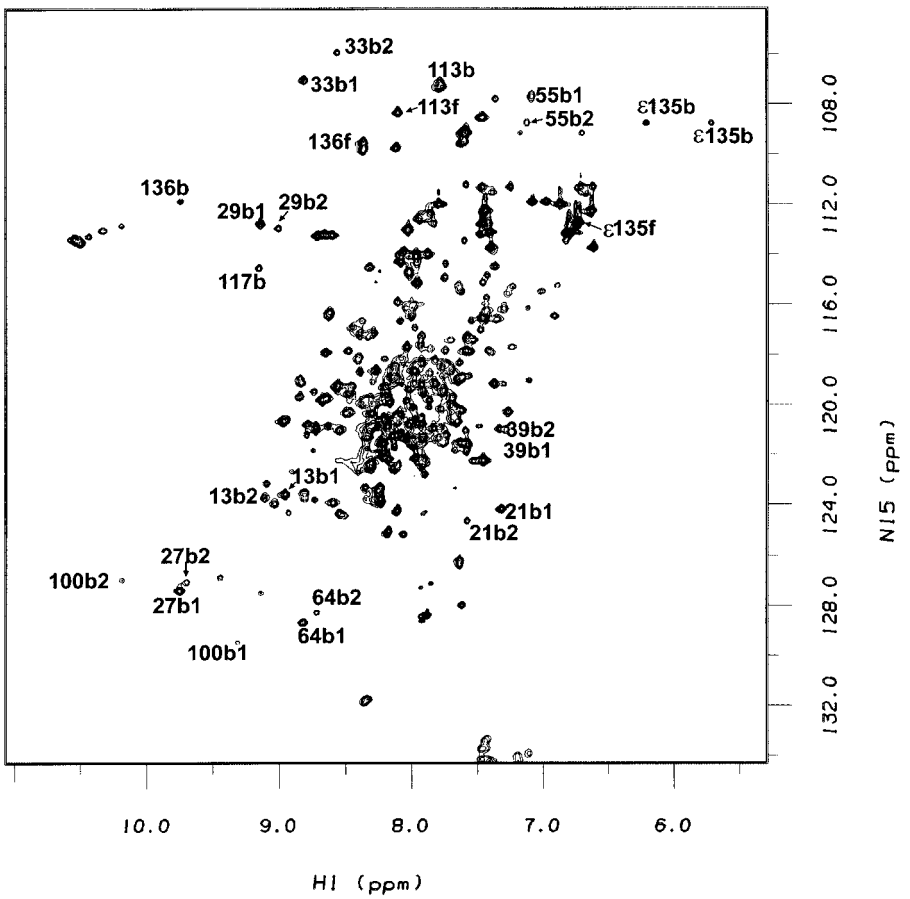

FIGURE 5: 2D $^1H-^{15}N$ HSQC spectrum of uniformly ^{15}N-labeled CaM(V136G) at 25 °C at a $[Ca^{2+}]/[CaM]$ ratio of 7. The assignments of several residues to signals corresponding to the different Ca^{2+}-bound species are indicated in the spectrum. For site I, II, and III residues, the Ca_3-CaM signals are designated as b1 and the Ca_4-CaM signals are designated as b2. For site IV residues, the Ca_3-CaM signals are designated as f (Ca^{2+} free) and the Ca_4-CaM signals are designated as b (Ca^{2+} bound).

Ile100 (Ile100b2) appeared in slow exchange with the previous Ca^{2+}-bound Ile100 signal (Ile100b1) and with the apo Ile100f signal (see Figure 4). The new Ile100b2 signal is at the known position of Ile100 in the spectrum of wild-type Ca_4-CaM. Simultaneously with the appearance of this peak, a new signal emerged at a $[Ca^{2+}]/[CaM]$ ratio of 3.3 that can be assigned to the mutated residue Gly136 in its Ca^{2+}-bound form at 9.86 ppm/113.31 ppm for $\delta(^1H)/\delta(^{15}N)$. It is worth noting that there is an appreciable deshielding of the ^1H nuclei for both Ile100b2 and Gly136b compared with Ile100b1 and Gly136f; such deshielding (*45*) is an indication that the intradomain β-sheet hydrogen bonds involving the two position 8 residues in the C-domain have been formed on going from the site IV unfolded Ca_3-CaM (species C) to the site IV folded Ca_4-CaM species (species D in Scheme 1).

Above this $[Ca^{2+}]/[CaM]$ ratio of 3.3, many other C-domain signals appeared at their known positions for wild-type Ca_4-CaM, indicating the presence of a Ca_4-bound species of the mutant CaM(V136G) with its calcium-bound site IV binding loop folded with a conformation similar to that of wild-type CaM (species D in Scheme 1). This can be seen for other residues corresponding to calcium-binding loop IV, such as (NH^{ϵ}_2) signals for residue Gln135, and also for residues corresponding to the N-domain, such as the NH of Gly33 at 8.53 ppm (signal G33b2). This signal was in slow conformational exchange with signal G33b1 at 8.75 ppm. It can be seen in Figure 5 that several N-domain residues have an additional calcium-bound signal (b2 signals): these include Lys21, Ile27, Thr29, Val35, and Leu39 (calcium-binding loop I) and Asn60 and Asp64 (calcium-binding loop II). The fact that several N-domain residues gave two signals corresponding to different calcium-bound forms of the C-domain indicated that in at least one of the forms there is an interaction between the two domains. It is proposed that this involves the Ca^{2+}-bound N-domain interacting with C-domain residues in the unfolded Ca^{2+}-free site IV (see species C in Scheme 1). Upon binding calcium to site IV, the mutant Ca_4-CaM can adopt a nativelike conformation (species D); by analogy with wild-type CaM (*6*, *42*) it is inferred that there is no direct interaction between the folded domains in this state.

Conformational Exchange Cross-Peaks. Exchange between signals arising from the same residue in different species was detected using ROESY−HSQC experiments to distinguish between magnetization transfer effects arising from dipolar relaxation and from conformational exchange (Figure 6). Since dipolar and exchange ROESY cross-peaks have opposite phases (*46*), this is a straightforward method for linking signals in conformational exchange arising from the same residue.

In the ROESY−HSQC spectra obtained for the CaM-(V136G) mutant the presence of exchange cross-peaks indicated slow exchange on the NMR time scale between the different species containing two (sites I and II), three (sites I, II, and III), or four (sites I, II, III, and IV) calcium

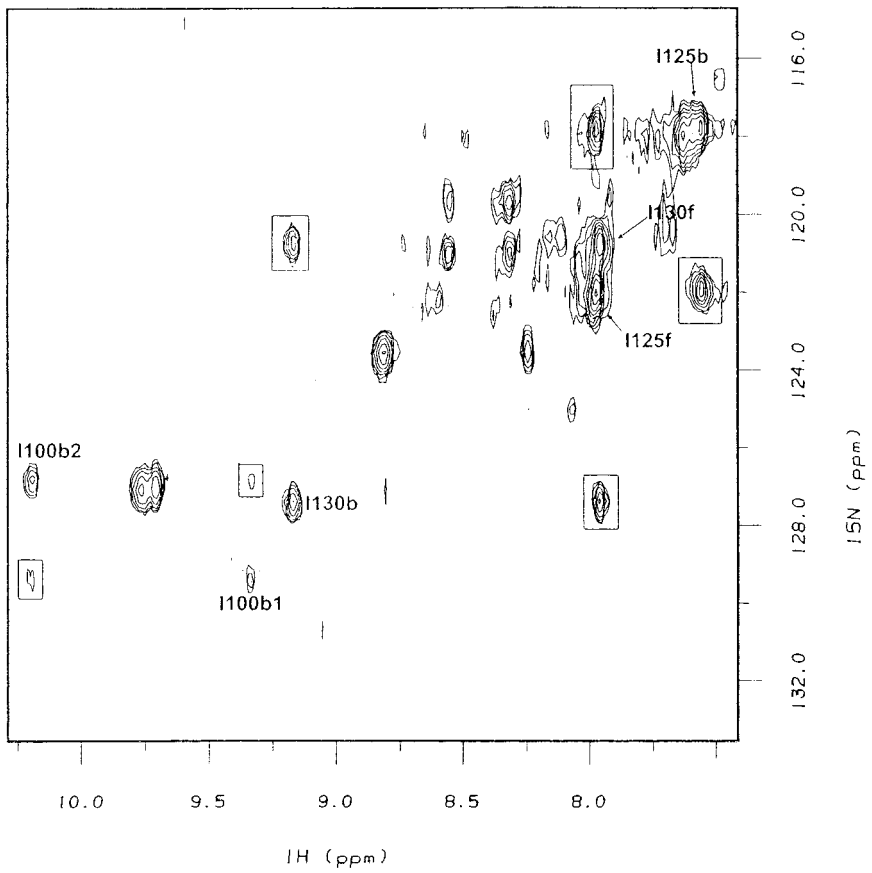

FIGURE 6: A region of the 2D $^{1}H-^{15}N$ HSQC−ROESY spectrum of the selectively ^{15}N-Ile-labeled mutant CaM(V136G) at a $[Ca^{2+}]$/[CaM] ratio of 7 and 25 °C showing the exchange signals enclosed in boxes.

ions at different $[Ca^{2+}]$/[CaM] ratios. The narrow signals from the unfolded parts of the C-domain were present during the whole titration but decreased in intensity as the Ca^{2+} concentration increased. No exchange cross-peaks were detected between N-domain signals and the narrow signals from residues in unfolded regions, consistent with the picture that the N-domain is fully folded in both its Ca^{2+}-free and its Ca^{2+}-bound states throughout the calcium titration.

At a $[Ca^{2+}]$/[CaM] ratio of 7, ROESY−HSQC experiments carried out with the mutant protein showed that even at this high concentration of calcium there were narrow signals from an unfolded conformation in exchange with signals from residues in a folded form of the C-domain. Signals from Ca^{2+}-bound site IV residues, such as signal Gly136b, continued to show exchange with an unfolded signal (Gly136f) even up to a $[Ca^{2+}]$/[CaM] ratio of 18. This is a reflection of the fact that under these conditions a substantial amount (70 ± 10%) of the site IV binding loop remains unfolded. At a $[Ca^{2+}]$/[CaM] ratio of 7, exchange cross-peaks were also detected between signals of site III residues, such as Ile100 in its Ca^{2+}-bound conformations (Ile100b1 and Ile100b2). However, no exchange cross-peaks were detected involving site III unfolded signals even though 20 ± 10% of the site III unfolded form was expected to be still present. The Ile100b1 and Ile100b2 signals were broad, and exchange signals with a small amount of site III unfolded form would be difficult to detect.

Temperature Dependence of Calmodulin Stability. The thermal stability of the mutant CaM(V136G) at a $[Ca^{2+}]$/[CaM] ratio of 7 was investigated by NMR. $^{1}H-^{15}N$ HSQC spectra were collected at 5 °C intervals over the temperature range increasing from 5 °C to 45 °C and then cooling to 5 °C. The temperature dependences of the intensities of the calcium-bound NH signals from residues Ile27, Asp64, Ile100, and Gly136 in their Ca^{2+}-bound positions (Ile27b1, I27b2, Asp64b1, Asp64b2, Ile100b1, Ile100b2, and Gly136b) are shown in Figure 7. Similar patterns of intensity changes were observed for other residues in corresponding regions of the protein. Asp64 was examined rather than Ile63 because the latter does not show separate b1 and b2 signals at a $[Ca^{2+}]$/CaM ratio of 7.

The temperature dependences of the signals plotted in Figure 7 can be used as typical examples illustrating the temperature behavior of N- and C-domain residues.

(i) The N-domain residues Ile27 and Asp64 each give rise to NH signals in two positions (signals b1 and b2) at 5 °C and a $[Ca^{2+}]$/[CaM] ratio of 7, and these are in slow exchange over the complete temperature range studied. The N-domain is fully folded at this calcium concentration. Both residues showed a very similar temperature dependence. As the temperature was raised, the b1 signals (from the Ca_2-CaM species B and Ca_3-CaM species C) increased whereas the intensity of b2 signals (from the Ca_4-CaM species D) decreased and had disappeared completely at 45 °C. This is consistent with the unfolding of the Ca^{2+}-bound C-domain with increasing temperature and the stability of the Ca^{2+}-bound N-domain over this temperature range (*29*).

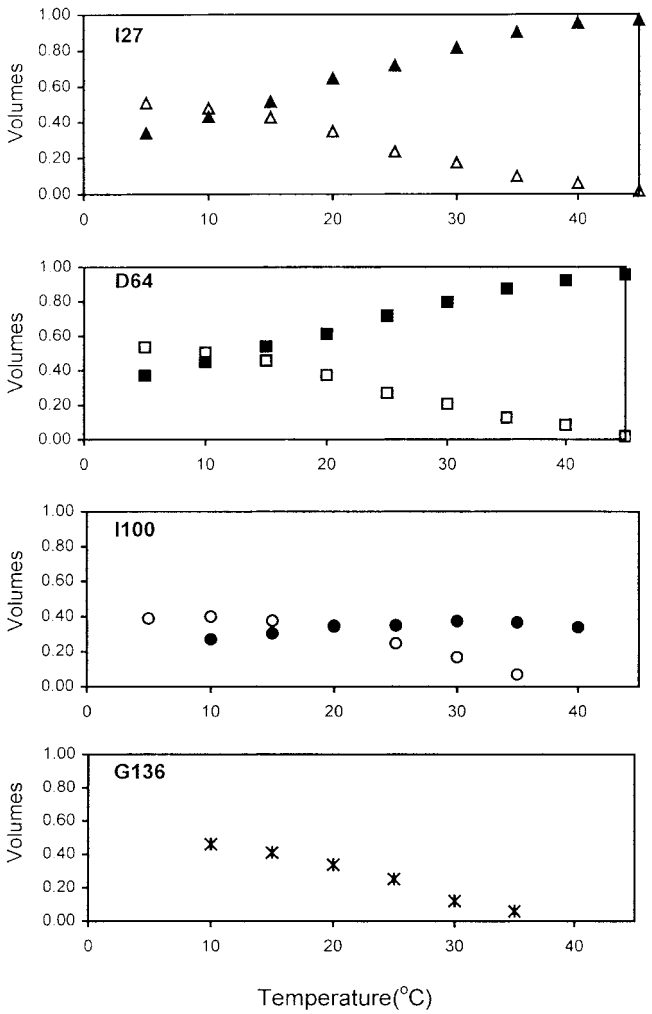

FIGURE 7: Temperature dependence plots for signals from residues Ile27b1 (▲), Ile27b2 (△), Asp64b1 (■), Asp64b2 (□), Ile100b1 (●), Ile100b2 (○), and Gly136b (∗) in their Ca^{2+}-bound conformations measured using a uniformly ^{15}N-labeled sample of CaM(V136G) at a $[Ca^{2+}]/[CaM]$ ratio of 7. The data for Gly136f were not included because this signal overlaps the Gly134 signal. The curves were normalized according to $I_{obs}/(I_{total})_{max}$.

(ii) The Ile100 Ca^{2+}-bound b2 signals (from the Ca_4-CaM species D) decreased on increasing the temperature whereas the b1 signal (from the Ca_3-CaM species C) increased initially but decreased above 30 °C. This is consistent with the behavior observed for the N-domain residues. The Ile100 signal for Ca_2-CaM species B (not monitored) would increase with increasing temperature, thus explaining the decrease in signal intensity for Ile100b1 above 30 °C.

(iii) The C-domain residue Gly136 showed two signals in slow exchange between its Ca^{2+}-bound (folded) and Ca^{2+}-free (unfolded) positions (Gly136b and Gly136f, respectively). As the temperature was increased, the intensity of the Gly136b signal for the Ca_4-saturated species D decreased and disappeared completely at 40 °C, whereas the intensity of the Gly136f signal from the unfolded form increased with increasing temperature (quantitative measurements were not made because of overlap with Gly134f).

The V136G mutation reduces the stability of the C-domain and apparently decreases its affinity for Ca^{2+} at higher temperatures. For example, the Asp64b2 and Gly136b signals, reflecting the calcium(III,IV)-bound folded conformation (species D), decreased in intensity as the temperature was raised, reflecting a reduction in the amount of the folded C-domain present in solution (the Ca_4-CaM species). As the temperature was increased, the equilibrium between the calcium(III,IV)-bound folded form of the C-domain (species D) and the calcium(III)-bound partially unfolded form of the C-domain (species C) was shifted toward the partially unfolded conformation. The calcium(III,IV)-bound folded C-domain conformation of the mutant (V136G) as monitored by signals Ile100b2 and Gly136b disappeared completely at 40 °C. In contrast, the Ca^{2+}-bound C-domain of wild-type CaM only undergoes complete unfolding at temperatures above 90 °C (*29*). The complete reappearance of the mutant CaM C-domain signals as the temperature is lowered indicates that the temperature-induced unfolding transition of the C-domain is fully reversible (*29*).

Complex of V136G CaM with Ca^{2+} and a sk-MLCK Peptide. The $^1H-^{15}N$ HSQC spectrum of the complex of ^{15}N-labeled V136G CaM formed with the sk-MLCK 26-residue peptide at a $[Ca^{2+}]/[CaM]$ ratio of 7 at 25 °C showed chemical shifts similar to those for the corresponding complex formed with wild-type CaM and showed no signals corresponding to unfolded residues. This indicates that for this CaM−peptide complex the wild-type and mutant proteins have the same (or very similar) folded conformation. This confirms the earlier study of Browne et al. (*29*) ,who noted that the site IV mutant adopts a folded conformation in the presence of calcium and the sk-MLCK peptide. Other calmodulin calcium-binding site mutants (involving the conserved bidentate glutamate ligand at loop position 12) have also been shown to recover the folded structure only upon binding sm- or sk-MLCK target peptides (*24*, *26*).

DISCUSSION

Ca^{2+} Binding to CaM(V136G). The binding of Ca^{2+} to wild-type CaM has been well studied by several techniques. In NMR experiments, the chemical shifts of the amide ^{15}N signals of the residues in position 8 of each of the four Ca^{2+}-binding loops have been shown to be site-specific probes for Ca^{2+} binding (*30*). By following the evolution of these signals throughout a Ca^{2+} titration, one can monitor the binding of Ca^{2+} at each of the four binding sites.

For wild-type CaM, the Ca^{2+} ion has a higher affinity for the C-domain sites (III and IV) than for the N-domain sites (I and II) (*8*). The binding to the C-domain sites usually results in slow-exchange conditions for the free and bound signals while the binding to the lower affinity N-domain sites results in fast exchange (*30*). Measurements of the stoichiometric association constants for wild-type CaM and its tryptic fragments (*19*, *47*) showed that the stoichiometric Ca^{2+}-binding constants for C-domain binding are about five times larger than those for the N-domain. These characteristics result in the Ca^{2+}-binding curves of the two domains overlapping significantly, with the Ca^{2+} binding to the N-domain starting before all of the sites in the C-domain are occupied (*30*, *47*).

The present NMR studies show that the calcium-binding behavior of the mutant CaM(V136G) contrasts with that of wild-type CaM in two important aspects. First, Ca^{2+} clearly binds initially to the N-domain sites, and there is a decrease in the Ca^{2+}-binding constant for both site III and site IV correlating with the structural destabilization of the C-domain

in the mutant CaM. Second, in contrast to wild-type CaM behavior, the NMR signals (Ile27 and Ile63) used to monitor Ca^{2+} binding to the N-domain of CaM(V136G) show slow-exchange conditions between Ca^{2+}-bound and Ca^{2+}-free species, indicating that the Ca^{2+} binding is tighter than to the N-domain of the wild-type CaM (assuming that the on-rates have not changed). This observation is surprising since the N-domain sequence is identical in both the wild-type and the mutant calmodulins, and therefore one would expect the Ca^{2+}-binding behavior of this domain to be identical in the two proteins if there are no interactions between the domains. The increased affinity of the N-domain sites explains why the stoichiometric association constants for Ca^{2+} binding to V136G are similar to those of the wild type (*29*). It is known that the Ca^{2+} affinity of CaM sites is increased substantially by interactions with target peptides (*13*, *48*), and similar interactions between the folded N-domain and unfolded parts of the C-domain would offer an explanation for the increased Ca^{2+}-binding affinity of the N-domain sites in the mutant.

As was found in the wild-type CaM, Ca^{2+} binds to the C-domain of the mutant in slow exchange, indicating that the dissociation rate constants could be fairly similar in the two proteins. However, the Ca^{2+} association rates may also be very different because these require formation of the folded state of the C-domain before Ca^{2+} can bind.

Intradomain Cooperativity of Ca^{2+} Binding. The binding of two Ca^{2+} ions to each pair of EF-hands in the N- and C-terminal domains of wild-type calmodulin has been found to show positive cooperativity (*47* and references therein). Two sets of interactions play crucial roles in bringing the paired EF-hands together and result in the folding of the domain. One involves formation of the hydrophobic core of each domain, for which the hydrophobic side chain of the residue in position 8 appears to be very important. The other interaction involves stabilization of the cycle of cooperative interactions across the β-sheet upon Ca^{2+} binding to both paired sites (*3*, *49*), when the backbone C═O and N−H groups of the residue in position 8 are involved in forming hydrogen bonds between the strands. The V136G mutation of the position 8 residue is a good probe for assessing the different influences of these two sets of interactions since this mutation alters the capacity of this residue to contribute to the hydrophobic core but does not remove its capacity to form a cycle of cooperative interactions connecting the Ca^{2+} ions across the β-sheet.

For the mutated C-terminal domain, lowered affinities were deduced from the NMR experiments for both of the C-domain Ca^{2+}-binding sites as compared with the wild-type C-domain sites. The fact that both sites in the mutated C-domain have lowered affinities indicates the strong interdependence of the Ca^{2+} affinities with the local structural stability of the paired binding loops. The NMR results also clearly show the formation of the site III calcium-occupied species (species C in Scheme 1) preceding the formation of the Ca_4-CaM species (species D), suggesting a reduction in the apparent cooperativity relative to wild-type CaM. No evidence was found for site IV binding calcium in the absence of calcium binding to site III (the only detected C-domain NMR signals correspond to species with site III occupied or sites III and IV occupied but none for species having only site IV occupied). Although the V136G mutation has not removed any of the calcium-liganding groups of site IV, the presence of the hydrophobic side chain of the residue in position 8 appears to be essential for ensuring the integrity of the domain structure that promotes the correct fold for binding of Ca^{2+} to site IV in the C-domain. The fact that Ca^{2+} appears to bind to site IV only in the presence of an occupied site III implies that there could be some cooperative binding in the mutant. This would be consistent with the presence of the cycle of cooperative interactions connecting the Ca^{2+} ions across the β-sheet as indicated by the ^1H chemical shift evidence for hydrogen bonding involving the Ile100 NH (to the Gly136 C═O group) and the Gly136 NH (to the Ile100 C═O group) on forming the mutant Ca_4-CaM species (Figure 5).

Insights into the Folding Process of Calmodulin. Residues in position 8 of each of the four calcium-binding loops (I27, I63, I100, V136) are highly conserved in the calmodulin superfamily of proteins and form part of the hydrophobic core of the N-domain (I27, I63) and the C-domain (I100, V136). A study of the site-directed mutagenesis of residue Val136 offers a possible method for dissecting out the contribution of the valine side chain to the stability and folding of calmodulin. Identifying situations in which incorrect as well as correct folding of a polypepetide chain occurs can provide important information about the factors influencing the efficient attainment of the closely packed fully folded structure for the native protein. NMR is a useful method for examining the conformations of unfolded and partly folded proteins.

For the Ca^{2+}-free state of the mutant V136G calmodulin, the $^1H-^{15}N$ HSQC spectrum shows that the mutation gives rise to an unfolded C-domain at 25 °C. This indicates the importance of the hydrophobic side-chain contacts between the two residues in position 8 for the structural stability of CaM. This mutation has a significant influence on the formation of the hydrophobic core involving the C-domain polypeptide chain, indicating that formation of these side-chain interactions provides a central mechanistic step in the folding of each calmodulin domain.

The addition of Ca^{2+} to the apo mutant calmodulin has two effects. Initially, Ca^{2+} binds to the nativelike N-domain (species A in Scheme 1) and thus changes its conformation from a "closed" apo state to an "open" holo state, exposing the hydrophobic pocket of the domain that is known to bind to hydrophobic "anchors" of calmodulin-binding target protein sequences (*4*, *9*−*11*). Subsequently, the addition of more Ca^{2+} induces folding of the calcium-binding loops in the C-domain of the mutant CaM. When Ca^{2+} binds to both sites III and IV, it shifts the population of molecules toward the fully native-like folded conformation (species D in Scheme 1). However, even at high ratios of $[Ca^{2+}]/[CaM]$ of up to 18 only about 55% of the mutant calmodulin has the native-like folded conformation (with sites I, II, III, and IV occupied), and this coexists in solution with partially unfolded forms of the C-domain. This slow exchange behavior between Ca^{2+}-free and Ca^{2+}-bound forms of the C-domain suggests that the intrinsic affinity of Ca^{2+} for the folded C-domain is relatively high in the mutant (the overall affinity being low because of the much reduced on-rate). Starovasnik et al. (*31*) have interpreted similar slow-exchange behavior for C-domain signals in Ca^{2+} titrations of the E140Q calmodulin mutant in terms of a slow conformational change induced by the Ca^{2+} binding.

The mutated C-domain, lacking the hydrophobic cluster that appears to be fundamental for ensuring its correct native folding, is observed as a mixture of different conformations ranging from extended to nativelike folds (corresponding to the occupation of sites I and II, sites I, II, and III, and sites I, II, III, and IV). The population of the fully folded form in this mixture (species D) increases as the [Ca^{2+}]/[CaM] ratio increases. It was found previously by CD (*29*) that even a 100-fold molar excess of Ca^{2+} gives only a partial restoration of the mutant C-domain to the wild-type conformation, and recent work shows that this persists up to an $\sim 10^4$-fold molar ratio (S. R. Martin, L. Masino, and P. M. Bayley, unpublished results). Hence, some incompletely folded forms of the CaM(V136G) mutant are evidently still present at very high [Ca^{2+}]/[CaM] ratios.

Interaction between the Two Domains. In wild-type Ca_4-CaM in solution, the two domains are known to have a degree of orientational freedom with respect to each other (*6*, *50*) and to present a larger radius of gyration than Ca_4-CaM−peptide complexes (*14*). Hence, any interactions between the folded domains of wild-type Ca_4-CaM are likely to be relatively unspecific. In Ca^{2+} titration experiments with wild-type calmodulin there was no indication that the chemical shifts of NMR signals from residues in one domain were influenced by Ca^{2+} binding to the other domain (*30*).

In the present work on mutant CaM(V136G) there is clear experimental evidence for an interaction between the N- and C-domains at intermediate levels of calcium saturation. Several N-domain residues show an additional signal in slow exchange with the original signal in the spectra of the calmodulin mutant at [Ca^{2+}]/[CaM] ratios between 1.6 and 40. It is clear from the presence of two signals arising from N-domain residues that the environments of these residues are sensitive to the conformational change of the C-domain occurring when Ca^{2+} binds to the C-domain. As the temperature is lowered, the intensities of the N-domain b2 signals increase in parallel with the intensities of C-domain signals assigned to the folded form (b2 for site III and b for site IV). This supports the view that the b2 signals of the N-domain are reflecting the presence of a folded C-domain which no longer has the capability of providing an interdomain interaction with the N-domain (species D in Scheme 1).

Earlier studies (*13*, *48*) showed that for wild-type calmodulin the calcium affinity of both domains is enhanced by interactions with calmodulin-binding target proteins. It is plausible that similar interactions generally involving a combination of hydrophobic and basic residues could be responsible for the increased Ca^{2+} affinity of the N-domain of the mutant calmodulin as compared with the wild type. This could arise, for example, from interactions of the N-domain with hydrophobic side chains from the unfolded regions of the C-domain or from direct interactions involving basic residues on the N-domain with acidic residues in the unfolded C-domain. Since the V136G mutation destabilizes the whole hydrophobic core of the C-domain, it is likely that there are a number of residues potentially available for hydrophobic interaction with the N-domain. Addition of the sk-MLCK peptide to the mutant CaM results in only the Ca_4-CaM fully folded form being present, and this is consistent with the interdomain interactions being replaced by interactions with the target sk-MLCK peptide.

Recent urea-induced unfolding experiments based on CD and UV measurements on apo wild-type CaM *(51)* indicate interactions between the folded N-domain and the unfolded C-domain in an equilibrium unfolding intermediate. In the presence of Ca^{2+} ions, a species involving interactions of the unfolded N-domain and the folded (holo) C-domain occurs as an intermediate in the urea unfolding. The existence of such an intermediate depends critically on the relative affinities of Ca^{2+} for the two domains (for wild-type CaM, Ca^{2+} binds more tightly to the C-domain than to the N-domain). In the case of the V136G mutant, stoichiometric Ca^{2+}-binding constants, based on optical spectroscopic measurements, did not resolve the relative affinities of the mutant C-domain and the nonmutated N-domain (*29*). The present NMR work has unequivocally shown that the N-domain binds calcium with a higher affinity than the mutant C-domain and that this affinity is greater than the wild-type N-domain in wild-type CaM. These effects, together with the detection of the resonances associated with the intermediate species observed as a function of the [Ca^{2+}]/[CaM] ratios, provide evidence for the interaction of the holo N-domain with the mutant C-domain in CaM(V136G).

Nakashima et al. (*37*) have reported evidence that in yeast CaM the N- and C-domains interact with each other and influence the Ca^{2+}-binding affinities in the whole molecule: the yeast CaM only binds three Ca^{2+} ions and has a defective fourth Ca^{2+} binding site that may be involved in the interdomain interaction (*37*, *38*). From NMR studies of interactions between half-molecule fragments of Ca^{2+}-bound yeast CaM, Lee and Klevit (*38*) have obtained direct evidence that the two domains interact via their exposed hydrophobic surfaces. Several other studies of interdomain interactions in various CaMs and mutants have also been reported (*31*−*36*).

Comparison with Other Position 8 Mutants. Browne et al. found that for calmodulins with similar mutations at the other position 8 residues in loops I, II, and III (namely, I27G, I63G, and I100G, respectively) the addition of Ca^{2+} restores the native fold (*29*) as judged by near- and far-UV CD. This is not the case for CaM(V136G), since although the addition of Ca^{2+} yields the native fold to some degree, it is unable to fully displace the equilibrium to the completely folded form even at ratios of [Ca^{2+}]/[CaM] up to 100. This behavior can be rationalized in terms of the interdomain interactions described above. For the V136G CaM, the unfolded site IV EF-hand has been shown to interact with the Ca^{2+}-bound N-domain, and this would result in stabilizing the unfolded form of the mutant which does not have the correct fold for binding Ca^{2+}. This interdomain interaction would appear to be favored when one is dealing with a C-terminal EF-hand site and a C-terminal α-helix (residues 139−148) (as for site IV) rather than an internal EF-hand (as for site III in the I100G CaM mutant). This would offer an explanation for the V136G mutant being more resistant to refolding in the presence of Ca^{2+} than is the I100G mutant.

In contrast to the CaM(V136G) mutant, both position 8 N-domain mutants I27G and I63G have been observed to completely refold on addition of Ca^{2+}. This may reflect the greater probability of domain unfolding due to the proximity of residue 136 to the C-terminus of CaM and the greater stability of the N-domain compared to the C-domain in apo wild-type CaM (*51*−*54*).

Concluding Remarks. The NMR measurements presented here for the V136G calmodulin mutant provide a more detailed account of the molecular events that occur during folding than do similar measurements on wild-type calmodulin. The individual domains of wild-type calmodulin fold and unfold rapidly in apparently two-state reactions, with no observable intermediate states (S. R. Martin, L. Masino, C.-R. Rabl, and P. M. Bayley, in preparation). The loss of an essential hydrophobic residue such as Val136 leaves the folding of the mutated C-domain incomplete, allowing access to a wealth of molecular events that normally cannot be parametrized. The detailed nature of the observed NMR data provides insights into a whole range of dynamic processes and interactions defining the conformational landscape for this calmodulin mutant in solution that cannot be obtained by any other method. In the present work, the use of the whole CaM molecule rather than the individual domains has proved to be particularly interesting for this type of study since the effects of the point mutation on domain−domain interactions could be investigated. Remarkably, this single-point mutation of the C-domain increases the Ca^{2+} affinity of the nonmutated N-domain and also stabilizes an unfolded state of the protein. The results of this study can be extended for the interpretation of the molecular processes underlying the overall behavior of related mutants (*29*).

ACKNOWLEDGMENT

The NMR experiments were carried out at the MRC Biomedical NMR Centre, Mill Hill, and we thank Drs. Tom Frenkiel and Fred Muskett for their help and advice with the NMR experiments. We are grateful to Dr. Kathy Beckingham (Rice University, Houston, TX) for supplying the original pOTSNco12 vector containing the cDNA coding for *D. melanogaster* calmodulin and to Peter Browne for the original cloning of the wild-type calmodulin and the CaM(V136G) mutant and for his expert technical assistance.

REFERENCES

1. Cohen, P., and Klee, C. B., Eds. (1988) *Molecular Aspects of Cell Regulation: Vol. 5: Calmodulin*, Elsevier, New York.
2. Kawasaki, H., and Kretsinger, R. (1994) *Protein Profile 1*, 343−517.
3. Strynadka, N. C. J., and James, M. N. G. (1989) *Annu. Rev. Biochem. 58*, 951−998.
4. Crivici, A., and Ikura, M. (1995) *Annu. Rev. Biophys. Biomol. Struct. 24*, 85−116.
5. Babu, Y. S., Sack, J. S., Greenhough, T. J., Bugg, C. E., Means, A. R., and Cook, W. J. (1985) *Nature 315*, 37−40.
6. Barbato, G., Ikura, M., Kay, L. E., Pastor, R. W., and Bax, A. (1992) *Biochemistry 31*, 5269−5278.
7. Kretsinger, R. H. (1976) *Annu. Rev. Biochem. 45*, 239−266.
8. Klevit, R. E., Dalgarno, D. C., Levine, B. A., and Williams, R. J. (1984) *Eur. J. Biochem. 139*, 109−114.
9. Finn, B. E., Evenäs, J., Drakenberg, T., Waltho, J. P., Thulin, E., and Forsén, S. (1995) *Nat. Struct. Biol. 2*, 777−783.
10. Kuboniwa, H., Tjandra, N., Grzesiek, S., Ren, H., Klee, C. B., and Bax, A. (1995) *Nat. Struct. Biol. 2*, 768−776.
11. Zhang, M., Tanaka, T., and Ikura, M. (1995) *Nat. Struct. Biol. 2*, 758−767.
12. Rhoads, A. R., and Friedberg, F. (1997) *FASEB J. 11*, 331−340.
13. Bayley, P. M., Findlay, W. A., and Martin, S. R. (1996) *Protein Sci. 5*, 1215−1228.
14. Krueger, J. K., Bishop, N. A., Blumenthal, D. K., Zhi, G., Beckingham, K., Stull, J. T., and Trewhella, J. (1998) *Biochemistry 37*, 17810−17817.
15. Roberts, D. M., Crea, R., Malecha, M., Alvarado-Urbina, G., Chiarello, R. H., and Watterson, D. M. (1985) *Biochemistry 24*, 5090−5098.
16. Putkey, J. A., Draetta, G. F., Slaughter, G. R., Klee, C. B., Cohen, P., Stull, J. T., and Means, A. R. (1986) *J. Biol. Chem. 261*, 9896−9903.
17. Beckingham, K. (1991) *J. Biol. Chem. 266*, 6027−6030.
18. Maune, J. F., Klee, C. B., and Beckingham, K. (1992) *J. Biol. Chem. 267*, 5286−5295.
19. Martin, S. R., Maune, J. F., Beckingham, K., and Bayley, P. M. (1992) *Eur. J. Biochem. 205*, 1107−1114.
20. Maune, J. F., Beckingham, K., Martin, S. R., and Bayley, P. M. (1992) *Biochemistry 31*, 7779−7786.
21. Evenäs, J., Thulin, E., Malmendal A., Forsén, S., and Carlström, G. (1997) *Biochemistry 36*, 3448−3457.
22. Evenäs, J., Malmendal, A., Thulin, E., Carlström, G., and Forsén, S. (1998) *Biochemistry 37*, 13744−13754.
23. Evenäs, J., Forsén, S., Malmendal A., and Akke, M. (1999) *J. Mol. Biol. 289*, 603−617.
24. Haiech, J., Kilhoffer, M. C., Lukas, T. J., Craig, T. A., Roberts, D. M., and Watterson, D. M. (1991) *J. Biol. Chem. 266*, 3427−3431.
25. Gao, Z. H., Krebs, J., VanBerkum, M. F. A., Tang, W. J., Maune, J. F., Means, A. R., Stull, J. T., and Beckingham, K. (1993) *J. Biol. Chem. 268*, 20096−20104.
26. Findlay, W. A., Martin, S. R., Beckingham, K., and Bayley, P. M. (1995) *Biochemistry 34*, 2087−2094.
27. Wu, X., and Reid, R. E. (1997) *Biochemistry 36*, 3608−3616.
28. Elhorst, B., Hennig, M., Forsterling, H., Diener, A., Maurer, M., Schulte, P., Schwalbe, H., Griesinger, C., Krebs, J., Schmid, H., Vorherr, T., and Carafoli, E. (1999) *Biochemistry 38*, 12320−12332.
29. Browne, J. P., Strom, M., Martin, S. R., and Bayley, P. M. (1997) *Biochemistry 36*, 9550−9561.
30. Biekofsky, R. R., Martin, S. R., Browne, J. P., Bayley, P. M., and Feeney, J. (1998) *Biochemistry 37*, 7617−7629.
31. Starovasnik, M. A., Su, D.-R., Beckingham, K., and Klevit, R. E. (1992) *Protein Sci. 1*, 245−253.
32. Pedigo, S., and Shea, M. A. (1995) *Biochemistry 34*, 1179−1196.
33. Mukherjea, P., Maune, J. F., and Beckingham, K. (1996) *Protein Sci. 5*, 468−477.
34. Shea, M. A., Verhoeven, A. S., and Pedigo, S. (1996) *Biochemistry 35*, 2943−2957.
35. Sorensen, B. R., and Shea, M. A. (1998) *Biochemistry 37*, 4244−4253.
36. Sun, H., Yin, D., and Squier, T. C. (1999) *Biochemistry 38*, 12266−12279.
37. Nakashima, K.-I., Ishida, H., Ohki, S.-Y., Hikichi, K., and Yazawa, M. (1999) *Biochemistry 38*, 98−104.
38. Lee, S. Y., and Klevit, R. E. (2000) *Biochemistry 39*, 4225−4230.
39. Cavanagh, J., Fairbrother, W. J., Palmer, A. G., III, and Skelton, N. J. (1996) *Protein NMR Spectroscopy*, Academic Press, New York.
40. Kay, L. E., Torchia, D. A., and Bax, A. (1989) *Biochemistry 28*, 8972−8979.
41. Delaglio, F., Grzesiek, S., Vuister, G. W., Zhu, G., Pfeifer, J., and Bax, A. (1995) *J. Biomol. NMR 6*, 277−293.
42. Ikura, M., Spera, S., Barbato, G., Kay, L. E., Krinks, M., and Bax, A. (1991) *Biochemistry 30*, 9216−9228.
43. Ikura, M., Kay, L. E., and Bax, A. (1990) *Biochemistry 29*, 4659−4667.
44. Reuben, J., and Fiat, D. (1969) *J. Chem. Phys. 51*, 4918−4927.
45. Szilágyi, L. (1995) *Prog. NMR Spectrosc. 27*, 325−443.
46. Bothner-by, A. A., Stephens, R. L., Lee, J., Warren, C. D., and Jeanloz, R. W. (1984) *J. Am. Chem. Soc. 106*, 811−813.
47. Linse, S., Helmersson, A., and Forsén, S. (1991) *J. Biol. Chem. 266*, 8050−8054.

48. Keller, C. H., Olwin, B. B., LaPorte, D. C., and Storm, D. R. (1982) *Biochemistry 21*, 156−162.
49. Biekofsky, R. R., and Feeney, J. (1998) *FEBS Lett. 439*, 101−106.
50. Biekofsky, R. R., Muskett, F. W., Schmidt, J. M., Martin, S. R., Browne, J. P, Bayley, P. M., and Feeney, J. (1999) *FEBS Lett. 460*, 519−526.
51. Masino, L., Martin, S. R., and Bayley, P. M. (2000) *Protein Sci. 9*, 1519−1529.
52. Tsalkova, T. N., and Privalov, P. L. (1985) *J. Mol. Biol. 181*, 533−544.
53. Tjandra, N., Kuboniwa, H., Ren, H., and Bax, A. (1995) *Eur. J. Biochem. 230*, 1014−1024.
54. Urbauer, J. L., Short, J. H., Dow, L. K., and Wand, A. J. (1995) *Biochemistry 34*, 8099−8109.

BI001772A